

MOL # 90654

**Title Page**

**19-Substituted benzoquinone ansamycin heat shock protein-90  
inhibitors: Biological activity and decreased off-target toxicity**

Chuan-Hsin Chang, Derek A. Drechsel, Russell R. A. Kitson, David Siegel, Qiang

You, Donald S. Backos, Cynthia Ju, Christopher J. Moody, and David Ross

Department of Pharmaceutical Sciences, Skaggs School of Pharmacy and

Pharmaceutical Sciences, University of Colorado Anschutz Medical Campus, Aurora,

Colorado (C-H.C., D.A.D., D.S., Q.Y., D.S.B., C.J., D.R.)

School of Chemistry, University of Nottingham, University Park, Nottingham, United

Kingdom (R.R.A.K., C.J.M.)

MOL # 90654

**Running Title Page**

***Running Title***

Novel Hsp90 inhibitors with decreased off-target toxicity

***Corresponding author***

David Ross Ph.D.

University of Colorado School of Pharmacy

Mail Stop C238

12850 E. Montview Blvd. V20-2132A

Aurora, CO 80045

Tel: 303-724-7265

Fax: 303-724-7266

E-mail: [david.ross@ucdenver.edu](mailto:david.ross@ucdenver.edu)

***Number of Text Pages: 31***

***Number of Tables: 2 (1 supplemental)***

***Number of Figures: 8 (5 supplemental)***

***Number of References: 32***

***Words in Abstract: 250***

MOL # 90654

***Words in Introduction: 734***

***Words in Discussion: 1,053***

***List of Non-Standard Abbreviations:***

BQA: benzoquinone ansamycin

19BQA: 19-substituted benzoquinone ansamycin

Hsp: heat shock protein

GA: geldanamycin

17-AAG: 17-allylamino-17-demethoxygeldanamycin

17-DMAG: 17-(dimethylaminoethylamino)-17-demethoxygeldanamycin

NQO1: NAD(P)H:quinone oxidoreductase 1

HER2: human epidermal growth factor receptor 2

ES936: 5-methoxy-1,2-dimethyl-3-(4-nitrophenoxymethyl)indole-4,7-dione

MTT: 3-(4,5-dimethylthiazol-2-yl)-2,5-diphenyltetrazolium bromide

MOL # 90654

## Abstract

The benzoquinone ansamycins (BQAs) are a valuable class of antitumor agents that serve as inhibitors of heat shock protein-90 (Hsp90). However, clinical use of BQAs has resulted in off-target toxicities including concerns of hepatotoxicity. Mechanisms underlying the toxicity of quinones include their ability to redox cycle and/or arylate cellular nucleophiles at the unsubstituted 19-position of the molecule. We have therefore designed 19-substituted BQAs to prevent glutathione conjugation and non-specific interactions with protein thiols to minimize off-target effects and reduce hepatotoxicity. 19-Phenyl and 19-methyl substituted versions of GA and its derivatives, 17-AAG and 17-DMAG, did not react with glutathione, while marked reactivity was observed using parent BQAs. Importantly, while 17-DMAG induced cell death in primary and cultured mouse hepatocytes, 19-phenyl and 19-methyl DMAG showed reduced toxicity, validating the overall approach. Furthermore, our data suggest that arylation reactions rather than redox cycling are a major mechanism contributing to BQA hepatotoxicity. 19-phenyl BQAs inhibited purified Hsp90 in an NAD(P)H oxidoreductase 1 (NQO1)-dependent manner, demonstrating increased efficacy of the hydroquinone ansamycin relative to its parent quinone. Molecular modeling supported increased stability of the hydroquinone form of 19-phenyl-DMAG in the active site of human Hsp90. In human breast cancer cells,

MOL # 90654

19-phenyl BQAs induced growth inhibition also dependent upon metabolism via NQO1 with decreased expression of client proteins and compensatory induction of Hsp70. These data demonstrate that 19-substituted BQAs are unreactive with thiols, display reduced hepatotoxicity, and retain Hsp90 and growth inhibitory activity in human breast cancer cells although with diminished potency relative to parent BQAs.

MOL # 90654

## **Introduction**

The 90-kDa heat shock protein (Hsp90) is an evolutionarily conserved molecular chaperone that functions to promote the conformational stabilization and activation of a wide subset of client proteins. Many of these proteins are essential in transducing proliferative and survival signals and adaptive responses to stress. In cancer cells, Hsp90 can serve as a molecular chaperone to prevent the misfolding or degradation of numerous overexpressed or mutated oncoproteins including protein kinases, steroid receptors, and transcription factors. As a result, many cancers increasingly rely upon Hsp90 for growth, survival, and drug resistance (Whitesell and Lindquist, 2005). Inhibition of Hsp90 has attracted considerable interest in recent years as a potential therapeutic target for the development of a new generation of anti-cancer drugs that can block more than one cancer causing pathway (Workman, 2004). Increased expression of Hsp90 is associated with disease progression in melanoma, and diminished survival in breast, lung and gastrointestinal stromal tumors (Normant et al., 2011). Thus, targeting Hsp90 may effectively treat numerous cancer types.

Hsp90 uses ATP hydrolysis to assist in the folding of client proteins to their mature, correctly folded forms (Pearl and Prodromou, 2006). Preventing Hsp90 from performing its chaperone function through the inhibition of ATP binding has been accomplished by a structurally diverse group of compounds. Of these compounds the

MOL # 90654

benzoquinone ansamycins (BQAs) including geldanamycin (GA), were the original class of compounds identified (Whitesell et al., 1994). However, in preclinical studies GA demonstrated significant liver toxicity (Supko et al., 1995). Derivatives of GA, 17-allylamino-17-demethoxygeldanamycin (17-AAG), and 17-(dimethylaminoethylamino)-17-demethoxygeldanamycin (17-DMAG), have since emerged as candidate Hsp90 inhibitors. 17-AAG and 17-DMAG have progressed to Phase I and Phase II trials (Banerji et al., 2005; Modi et al., 2011; Pacey et al., 2011) and demonstrated activity in HER2-positive, trastuzumab-refractory breast cancer (Modi et al., 2011). 17-AAG is poorly soluble and requires specialized vehicles for formulation and administration, so the considerably more water soluble hydroquinone of 17-AAG (IPI-504) has been developed and is currently in clinical trials (Ge et al., 2006; Siegel et al., 2011). We have previously shown that hydroquinone ansamycins generated via NAD(P)H oxidoreductase 1 (NQO1) metabolism are more effective Hsp90 inhibitors than their respective parent quinones due to improved binding in the active site of Hsp90 (Guo et al., 2005).

Despite their clinical use, hepatotoxicity remains a problem with both 17-AAG and 17-DMAG. Hepatotoxicity of 17-AAG was found to be dose limiting in two separate Phase I trials (Banerji et al., 2005; Solit et al., 2007) and in the most recent Phase II trial in advanced unresectable breast cancer, five patients developed grade

MOL # 90654

3/4 toxicities which were primarily hepatic and pulmonary. Based on these toxicity findings and lack of efficacy, 17-AAG was not recommended for further study for this indication (Gartner et al., 2012). 17-DMAG also demonstrated significant toxicities in Phase I clinical trials including hepatotoxicity as reflected by changes in liver function (Pacey et al., 2011). The toxicity of quinones such as BQAs arises from their ability to redox cycle and/or arylate cellular nucleophiles (Ross et al., 2000). These molecules are capable of both redox cycling to produce reactive oxygen species and reaction with thiols at the 19-substituent, leading to the formation of glutathione conjugates and adducts with cellular proteins (Guo et al., 2008). We have therefore designed 19-substituted BQAs (19BQAs) to prevent thiol reactivity as an approach to minimize off-target effects and reduce hepatotoxicity of this class of Hsp90 inhibitors. We have previously described the synthesis of 19BQAs, protein crystallography establishing that these new compounds bind to Hsp90 with a favored *cis*-amide conformation for inhibition, and preliminary evidence for Hsp90 inhibition in cellular systems (Kitson et al., 2013).

The aim of this study was to validate that novel 19BQAs did not react with thiols, and to define their hepatotoxic potential relative to their parent unsubstituted quinones. 19-substitution of BQAs prevented nucleophilic attack of GSH and resulted in markedly reduced toxicity in freshly isolated hepatocytes, suggesting that arylation is



MOL # 90654

a major mechanism of hepatotoxicity. Using three separate approaches: a) purified NQO1, b) human breast cancer cells isogenic for NQO1, and c) molecular modeling, we also demonstrated that 19BQAs inhibit Hsp90 in an NQO1 dependent manner, emphasizing the importance of the hydroquinone ansamycin. Finally, our work shows that the 19BQAs are effective Hsp90 inhibitors and induce growth inhibitory effects in human breast cancer cells. When combined with diminished off-target toxicity, these novel 19BQA compounds may have a greater therapeutic window than their parent quinones.

MOL # 90654

## Materials and Methods

### Cell culture and reagents

17-Allylamino-17-demethoxygeldanamycin (17-AAG), geldanamycin (GA), 17-(dimethylaminoethylamino)-17-demethoxygeldanamycin (17-DMAG) were obtained from LC Laboratories (Woburn, MA); 19-Phenyl 17-AAG, 19-phenyl GA, 19-phenyl 17-DMAG, 19-methyl GA, 19-methyl 17-AAG, and 19-methyl 17-DMAG were synthesized as described (Kitson et al., 2013; Kitson and Moody, 2013), along with 5-methoxy-1,2-dimethyl-3-(4-nitrophenoxyethyl)indole-4,7-dione (ES936) (Guo et al., 2005). NADH, NADPH, 3-(4,5-dimethylthiazol-2-yl)-2,5-diphenyltetrazolium bromide (MTT), bovine serum albumin (BSA), Percoll, and mouse anti- $\beta$ -actin antibodies were obtained from Sigma Chemical Co. (St. Louis, MO). Yeast Hsp90 was obtained from Alexis (San Diego, CA). Recombinant human NQO1 (rhNQO1) was purified from *Escherichia coli* as described previously (Beall et al., 1994). The activity of rhNQO1 was 4.5  $\mu$ mol dichlorophenolindophenol/min/mg protein (Siegel et al., 2007). Malachite green phosphate assay kit was obtained from BioAssay Systems, Inc. (Hayward, CA). Mouse anti-Hsp70, rabbit anti-Hsp90 antibody and rabbit anti-Raf-1 antibodies were obtained from Enzo (Farmingdale, NY). Rabbit anti-Akt was from Cell Signaling (Beverly, MA). Purified mouse and human microsomes were purchased from BD

MOL # 90654

Biosciences (San Jose, CA).

### **Cell lines**

The human breast cancer cell lines MDA468 and BT474 were obtained from American Type Culture Collection (Manassas, VA). Parental MDA468 cells are NQO1 null due to homozygous expression of the NQO1\*2 polymorphism while the MDA468/NQ16 cell line was stably transfected with wild-type NQO1 (Dehn et al., 2004). Cells were grown in a humidified incubator at 37°C with 5% CO<sub>2</sub> in RPMI 1640 containing 10% (v/v) fetal bovine serum, (100 U/ml) penicillin, (100 µg/ml) streptomycin, and 4 mM glutamine. The murine TAMH hepatocyte cell line was provided by Christopher Franklin, Skaggs School of Pharmacy, University of Colorado and were maintained as described (Wu et al., 1994).

### **Polarographic Studies**

Oxygen consumption was measured using a Clark electrode following the addition of BQAs to NADPH- or NADH-supplemented human or mouse liver microsomes. Reactions (3 ml) were performed at 37°C in 50 mM potassium phosphate buffer, pH 7.4 containing 1 mg/ml bovine serum albumin, human or mouse liver microsomes (0.4 mg) and 50 µM BQA. Reactions were started by the addition of 0.5 mM NADH

MOL # 90654

or NADPH and oxygen consumption was measured over 5 min. Baseline oxygen consumption rates were determined following addition of DMSO and subtracted from measured rates with BQAs.

### **Reactions of BQAs with glutathione**

The conjugation of BQAs by glutathione was measured by HPLC following the incubation of BQAs with GSH in 50 mM potassium phosphate, pH 7.4 at 27°C. At the indicated times, reactions (1 ml) were stopped by the addition of acetic acid (15 µl) and directly analyzed by HPLC. Samples (50 µl) were separated at room temperature using a linear gradient (10 to 85 % buffer B over 12 min) on a reverse-phase C<sub>18</sub> (Luna II) column (5 µm, 4.6 x 250 mm, Phenomenex, Torrance, CA) using a flow rate of 1 ml/min and a detection wavelength of 270 nm. For HPLC analysis of GA and 17-AAG, the buffer system was: buffer A, 0.1% (v/v) trifluoroacetic acid; buffer B, acetonitrile, while for studies of 17-DMAG 50 mM ammonium acetate was used in place of 0.1% trifluoroacetic acid as buffer A.

### **Primary mouse hepatocyte isolation and liver toxicity assays**

Male C57BL/6 mice (8-10 weeks of age) were purchased from the Jackson Laboratory (Bar Harbor, ME) and kept in the Center of Laboratory Animal Care at the

MOL # 90654

University of Colorado Denver (UC Denver) for 1 week before sacrificing. All animal experiments were performed according to guidelines from the UC Denver Institutional Animal Care and use committee. Hepatocytes were isolated as previously described (Cheng et al., 2010; Yin et al., 2010) by collagenase perfusion, gravity sedimentations, and a final Percoll density gradient centrifuge step. The yield of hepatocytes was, on average,  $1 \times 10^7$  cells per liver with viability greater than 90%. Hepatocytes were plated in Williams' Medium E supplemented with 5 % FBS, 20 mM HEPES buffer with 2 mM of L-glutamine, 100 U/ml penicillin, and 100  $\mu$ g/ml streptomycin. Hepatocytes were seeded in 96-well plate at  $1 \times 10^4$  cells/well and allowed to adhere for 2 h before treatment with BQAs. Cells were exposed to 17-DMAG, or 19-phenyl and 19-methyl derivatives (range from 0-100  $\mu$ M) in Williams' Medium E for 24 h. At the end of the incubation, a 10  $\mu$ l aliquot of media was taken from each well to assess cytotoxicity via release of aspartate aminotransferase (AST). AST activity was measured using an assay kit (Teco Diagnostics, Anaheim, CA). Viability was also assessed using reduction of 3-(4,5-dimethylthiazol-2-yl)-2,5-diphenyltetrazolium bromide (MTT) to formazan (Guo et al., 2005; Guo et al., 2006)

TAMH cells were seeded in 96-well plate at  $1 \times 10^4$  cells/well and allowed to adhere overnight. Cells were exposed to 17-DMAG, or 19-phenyl and 19-methyl derivatives

MOL # 90654

(range from 0-100  $\mu$ M) in complete DMEM/F12 media for 72 h. At the end of incubation, BQAs were removed and viability was assessed using MTT assay and compared to cells at time-zero to determine LC<sub>50</sub> concentrations.

### **Heat shock protein 90 ATPase activity assay**

Inhibition of Hsp90 ATPase activity was measured as described previously (Guo et al., 2005). Briefly, purified yeast Hsp90 (2.5  $\mu$ g) was incubated in 100 mM Tris-HCl (pH 7.4) containing 20 mM KCl, 6 mM MgCl<sub>2</sub>, 400  $\mu$ M NADH, BQAs or 19BQAs with or without 3.3  $\mu$ g rhNQO1. Reactions (25  $\mu$ l) were started by the addition of 1 mM ATP and allowed to proceed at 37°C for 3 h. Reactions were then diluted with 225  $\mu$ l of 100 mmol/l Tris-HCl (pH 7.4) containing 20 mM KCl and 6 mM MgCl<sub>2</sub> mixed thoroughly, and 80  $\mu$ l were transferred to wells of a 96-well plate followed by 20  $\mu$ l malachite green reagent. After 10 min, trisodium citrate (83 mM) was added to stabilize the color and plates were read at 650 nm.

### **Computational-based molecular modeling**

All molecular modeling studies were conducted using Accelrys Discovery Studio 3.1 (Accelrys Software, Inc., San Diego, CA; <http://accelrys.com>). The structural coordinates for human Hsp90 (Sreeramulu et al., 2009) were obtained from the

MOL # 90654

protein data bank (<http://www.pdb.org>; PDB ID: 2K5B). The flexible docking algorithm (Koska et al., 2008), which allows for flexibility in both the ligand and the receptor, was used to predict the binding orientation of the quinone and hydroquinone forms of 19Ph-DMAG within the ATP binding site of Hsp90. Hsp90-ligand complexes underwent energy minimization *in situ* using the conjugate gradient method (10,000 iterations with a root mean square cutoff of 0.01 kcal/mol). The following residue side chains were designated as flexible in the calculations: Glu47, Asn51, Asp54, Lys58, Asp93, Met98, Asn106, Leu107, Lys112, Phe138, and Thr184. Ligand binding energies were calculated using the Poisson-Boltzmann implicit solvent model (Feig and Brooks, 2004).

### **Growth inhibition assay**

Growth inhibition in human breast cancer cell lines was measured using MTT assay as described previously (Guo et al., 2005). Briefly, cells were seeded at  $2 \times 10^3$  per well (96-well plate) in complete RPMI medium overnight. The next morning, the cells were treated with 19-phenyl BQAs, 19-methyl BQAs, and BQAs for 4 h, after which cells were rinsed free of drug and incubated in fresh medium for an additional 72 h.

### **Immunoblot analysis**

MOL # 90654

MDA468 and MDA468/NQ16 cells were grown in 100-mm plates in complete RPMI medium to approximately 70 % confluency. Cells were treated with DMSO, 19BQAs or BQAs (1-5  $\mu$ M) in 10 ml complete medium for 24 h. Following drug treatment, cells were washed in PBS and then lysed by the addition of RIPA lysis buffer (Boston Bioproducts, Ashland, MA) containing protease and phosphatase inhibitors and collected via scraping. Lysates were probe sonicated (10 seconds) on ice and then centrifuged at 13,000 rpm for 5 min at 4°C to remove cellular debris. Protein concentration was determined on supernatant by the method of Lowry et al. (Lowry et al., 1951). Samples were heated to 90°C in 2X Laemmli buffer, and protein (20  $\mu$ g) were separated by 12% SDS-PAGE (precast minigel, Bio-Rad, Hercules CA) and then transferred to 0.4- $\mu$ m polyvinylidene difluoride membranes. Membranes were blocked in 10 mM Tris-HCl (pH 8.0), 150 mM NaCl, 0.2% Tween 20, and 5% non-fat milk for a minimum of 1 h at room temperature. Anti-Hsp70, anti-Raf-1, and anti-Akt antibodies were incubated overnight at 4 degrees C. All primary antibodies were diluted 1:1,000 except  $\beta$ -actin (1:10,000). Horseradish peroxidase-labeled secondary antibodies (Jackson ImmunoResearch Labs, West Grove, PA) were diluted 1:10,000 and added for 60 min. Proteins were visualized using enhanced chemiluminescence detection. Quantitation of immunoblots from three independent experiments was performed using Adobe Photoshop 7.0.



MOL # 90654

### **Statistical analysis**

Statistical significance was determined using Prism 5.0 software (GraphPad Software Inc. San Diego, CA). Two-way ANOVA with concentration-group interaction were used for multiple comparisons with the application of SPSS v19.0 (SPSS, Inc., Chicago, IL, USA). Statistical significance was defined as  $p < 0.05$ .

MOL # 90654

## Results

### 19BQAs do not react with glutathione

19-substituted BQAs (Fig. 1) were synthesized as described previously (Kitson et al., 2013) in order to remove the potential for arylation of cellular thiols and proteins. We initially used 19-phenyl and 19-methyl substituted BQAs in these studies to provide proof of principle for this class of agents. Previously we had examined the reactivity of 19BQAs using a model thiol, N-acetylcysteine methyl ester with basic conditions, tetrahydrofuran and elevated temperatures (Kitson et al., 2013). The current experiments were performed using the biological thiol glutathione under physiological conditions. The reactivity of GA, 17-AAG, and 17-DMAG and their 19-substituted derivatives with glutathione was measured by HPLC. The parent quinones, (GA, 17-AAG, and 17-DMAG) readily formed glutathione adducts in the order of GA > 17-DMAG > 17-AAG as we and others have previously reported (Cysyk et al., 2006; Guo et al., 2008). However, 19-phenyl and 19-methyl substituted compounds of all three BQA series did not react with GSH (Fig. 2), thus validating the rationale for their synthesis.

### 19BQAs redox cycling rates compared to parent unsubstituted quinones.

MOL # 90654

We have shown previously that the BQAs in general have relatively low rates of redox cycling (Guo et al., 2008), but in the current study we have compared the relative rates of redox cycling of 19Ph- and 19Me-DMAG with the parent quinone, 17-DMAG. NADH or NADPH was used as a cofactor to provide reducing equivalents for one-electron reductases present in liver microsomes. The rates of oxygen consumption were measured as indicators of redox cycling rates of the studied compounds (Fig. 3A-D). In general, 19-phenyl substitution of 17-DMAG showed no difference in redox cycling rates relative to parent quinone, while 19Me-DMAG showed a significant decrease in rate. This was observed in NADH- and NADPH-supplemented human and NADPH-supplemented mouse liver microsomes. However, in NADH-dependent mouse liver microsomes, 19Me-DMAG consumed oxygen at a comparable rate to 17-DMAG and 19Ph-DMAG showed less oxygen consumption than DMSO controls (Fig. 3D).

### **19-substitution of BQAs reduces hepatotoxicity.**

Further studies were conducted with 19-substituted derivatives of 17-DMAG to evaluate hepatotoxicity of these compounds compared to the parent quinone. 17-DMAG exhibited dose-dependent toxicity in freshly isolated mouse hepatocytes (Fig. 4). However, 19Ph-DMAG and 19Me-DMAG showed reduced hepatotoxicity

MOL # 90654

compared to the unsubstituted parent quinone in terms of cell survival assessed using the MTT assay (Fig. 4A) and cytotoxicity via AST release (Fig. 4B). These results were confirmed in the mouse TAMH hepatocyte cell line: 17-DMAG was considerably more potent than 19Ph-DMAG and 19Me-DMAG in terms of growth inhibition and cell death (Table 1 and Supplementary Fig. 1). Specifically,  $IC_{50}$  and  $LC_{50}$  concentrations in TAMH cells were decreased 230- and 65-times, respectively with 19Ph-DMAG compared to the parent compound. 19Me-DMAG showed the least toxicity in TAMH cells with  $IC_{50}$  and  $LC_{50}$  concentrations 400- and 203-times lower, respectively than 17-DMAG. The fact that 19-substitution of 17-DMAG precludes GSH conjugation, yet shows no consistent relationship between toxicity and rates of redox cycling, and reduces damage to liver cells suggests that arylation reactions are a major contributing mechanism to the hepatotoxicity of BQAs.

### **Inhibition of Hsp90 by 19BQAs is NQO1-dependent**

We assessed the ability of 19BQAs to inhibit purified yeast Hsp90 ATPase activity using the malachite green ATPase activity assay. Previous data demonstrated that the Hsp90 inhibition induced by GA, 17-AAG, and 17-DMAG was dependent upon metabolism by NQO1, consistent with the greater inhibitory activity of the hydroquinone relative to the parent quinone (Guo et al., 2005). This data was

MOL # 90654

confirmed and extended to 19BQAs. Hsp90 ATPase activity was significantly decreased with both 19-phenyl BQAs and BQAs in the presence of NQO1 (Fig. 5).

Similar data was obtained using 19-methyl BQAs (Supplementary Fig. 2).

*In silico* molecular docking of 19Ph-DMAG into the active site of human Hsp90 supported the *in vitro* results. Although the binding orientations of both the 19-phenyl-quinone (Data Supplement: 2K5B&19phquinone) and 19-phenyl-hydroquinone (Data Supplement: 2K5B&19phhydroquinone) were not radically different, the hydroquinone form was predicted to form additional hydrogen bond interactions with Hsp90 compared with the parent quinone (Supplemental Fig. 3 and Supplemental Table 1). The hydroquinone form is predicted to form two additional hydrogen bond interactions with Asp54 and one with Asp93, while maintaining all of those hydrogen bonds involving the parent quinone. This likely plays a role both in the enhanced favorability of the predicted binding energy (-18.9 kcal/mol for the quinone versus -30.2 kcal/mol for the hydroquinone) and in the increased binding affinity observed *in vitro*.

### **19-phenyl BQAs induce growth inhibition with molecular biomarkers of Hsp90 inhibition in human breast cancer cell lines.**

To examine the role of NQO1 on Hsp90 inhibition ability and cytotoxicity of

MOL # 90654

19-substituted BQAs in human breast cancer, we used the BT474 and MDA468 cell lines. The MDA468 cell line was selected because it has no detectable NQO1 catalytic protein activity due to homozygous expression of the NQO1\*2 polymorphism. We have previously stably transfected the MDA468 cell line with a plasmid containing the human NQO1 coding region to generate an isogenic cell line (MDA468/NQ16) expressing a high level NQO1 protein and activity (Dehn et al., 2004) (Supplementary Fig. 4).

MDA468 or MDA468/NQ16 cells were treated with either 19-phenyl substituted BQAs or parent BQAs for 4 hours. Cells were then washed free of drug and growth inhibition was determined using the MTT assay after 72 h. All 19-phenyl derivatives and parent quinones showed greater growth inhibitory activity in NQO1-expressing MDA468/NQ16 cells, emphasizing the importance of the hydroquinone ansamycins to the Hsp90 inhibitory mechanism (Table 2). 19-phenyl substituted BQAs were also less potent than their respective parent quinones at inducing growth inhibition of MDA468/NQ16 cells. The  $IC_{50}$  values of all 19-phenyl derivatives and parent quinones in both MDA468 and MDA468/NQ16 cells are shown in Table 2 together with the fold increase in growth inhibition observed in cells containing high levels of NQO1. The role of NQO1 in growth inhibition induced by 17-DMAG and 19Ph-DMAG was further assessed in MDA468 and MDA468/NQ16 cells using the

MOL # 90654

mechanism based NQO1 inhibitor, ES936 (Guo et al., 2005). In these studies, cells were treated with either 17-DMAG or 19Ph-DMAG for 4 h in the presence or absence of ES936 pretreatment. Two-way ANOVA analysis demonstrated that growth inhibition caused by 19Ph-DMAG was significantly decreased by pretreatment with ES936 in MDA468/NQ16 cells. In contrast, pretreatment with ES936 had no effect on 19Ph-DMAG dependent growth inhibition in MDA468 cells (Fig. 6).

Expression levels of client proteins and Hsp70 were measured via immunoblot to confirm the molecular signature of cellular Hsp90 inhibition. Decreased levels of Hsp90 client proteins Raf-1 and Akt were observed with both 17-DMAG and 19Ph-DMAG in MDA468/NQ16 cells (Fig. 7A-B). Raf-1 and Akt were also decreased with 17-DMAG in NQO1-deficient MDA468 cells but to a lesser degree compared with MDA468/NQ16 cells. 19Ph-DMAG had little effect on Hsp90 client protein in NQO1-deficient MDA468 cells (Fig. 7C-D). A compensatory induction of Hsp70 was observed with both 17-DMAG and 19Ph-DMAG in MDA468/NQ16 and MDA468 cells. However, Hsp70 induction was more potent in MDA468/NQ16 cells, where over 4-fold increase in expression was observed compared to only a 2.2- or 1.6-fold increase in MDA468 cells with 17-DMAG or 19Ph-DMAG, respectively. Although immunoblotting and MTT growth inhibitory assays could not be performed under identical conditions due to cell number constraints, the NQO1-dependent

MOL # 90654

anti-cancer activity of BQAs and 19BQAs were apparent in both situations. In general, 17-DMAG showed slightly greater effects on clients at equimolar concentrations than 19Ph-DMAG itself consistent with the growth inhibitory data. GA, 17-AAG, and their 19-phenyl derivatives had similar NQO1-dependent effects on client protein degradation and Hsp70 induction. Consistent with their increased growth inhibitory capability, parent BQAs generally demonstrated greater potency (Supplementary Fig. 5)

To extend our results to a human epidermal growth factor receptor 2 (HER2)-positive human breast cancer cell line, we examined the effects of 19Ph-DMAG and 17-DMAG in BT474 cells. Both 19Ph-DMAG and 17-DMAG induced marked growth inhibition, with 17-DMAG demonstrating greater potency (Fig. 8A). These effects were reflected in decreased levels of Hsp90 client proteins upregulation of Hsp70 expression with both compounds (Fig. 8B-C). Changes in expression of Raf-1, Akt, and Hsp70 were similar with both 17-DMAG and 19Ph-DMAG, although 17-DMAG showed a significantly greater effect on HER2 degradation.



MOL # 90654

## Discussion

Hsp90 is a protein chaperone that promotes the maturation and conformational stabilization of cellular proteins important in transducing proliferation and survival signaling. It has evolved as a promising anticancer target since by blocking Hsp90, many client proteins which drive neoplasia can be simultaneously targeted, allowing a combinatorial anticancer blockade (Neckers and Workman, 2012; Workman et al., 2007). The BQA class of Hsp90 inhibitors have exhibited promising activity in Phase I and Phase II clinical trials but their development has been hindered by toxicity concerns, particularly hepatotoxicity (Banerji et al., 2005; Gartner et al., 2012; Pacey et al., 2011; Solit et al., 2007). This has led to the development of Hsp90 inhibitors using non-quinone scaffolds but these molecules may also be associated with their own characteristic toxicities (Rajan et al., 2011). In this work we have explored an alternative route to optimizing therapy employing Hsp90 inhibitors by examining mechanisms underlying the toxicity of the active class of BQA Hsp90 inhibitors and using chemical biology to minimize their toxicity and reduce off-target effects. The novel 19-substituted BQAs studied here showed reduced hepatotoxicity compared to their parent BQAs, but retain Hsp90 inhibitory and anti-cancer activity in human breast cancer cells.

Quinones induce biological toxicity as a function of their ability to arylate

MOL # 90654

biological nucleophiles and/or undergo redox cycling reactions to generate reactive oxygen species. BQA Hsp90 inhibitors such as GA, 17-AAG and 17-DMAG are known to interact with cellular thiols, including GSH, via addition at the electrophilic 19-position of the BQA molecule (Cysyk et al., 2006; Guo et al., 2008). In order to prevent the nucleophilic attack of thiols and other nucleophiles at the 19-position, we synthesized the 19-phenyl and 19-methyl derivatives of GA, 17-AAG and 17-DMAG. The details of the synthesis of these novel 19-substituted compounds are provided elsewhere (Kitson et al., 2013). In this work, we utilized 19-phenyl and 19-methyl derivatives as proof of principle that the 19-substituted BQAs as a class have potential as Hsp90 inhibitors with diminished off target toxicities and consequently, a greater therapeutic index. In contrast to their parent BQAs, 19-substituted derivatives did not react with cellular thiols such as glutathione, which validated the rationale for their synthesis. Hepatotoxicity has been a significant problem with the BQA Hsp90 inhibitors from their initial development as demonstrated by pre-clinical hepatotoxicity exhibited by GA up to the present day with the most recent phase II trial of 17-AAG demonstrating significant hepatotoxicity (Gartner et al., 2012). In order to determine whether reduced reactivity with thiols translated to reduced hepatotoxicity, we utilized a model employing freshly isolated mouse hepatocytes. In this system, marked dose-dependent toxicity could be observed using 17-DMAG, but

MOL # 90654

19-phenyl or 19-methyl substitution showed reduced toxicity in mouse hepatocytes. This is an important demonstration of decreased off target toxicity of the 19BQAs and is in agreement with previous data demonstrating lack of toxicity of these compounds in normal human umbilical vein endothelial cells (Kitson et al. 2012) Redox cycling can also contribute to quinone toxicity following one electron reduction with subsequent production of reactive oxygen species. In liver, microsomal NADPH cytochrome P450 reductase and NADH cytochrome b5 reductase are the predominant one electron reductases (Guo et al., 2008). Using mouse or human liver microsomes, we found no consistent relationship between toxicity and redox cycling of the 19-substituted DMAG series of compounds.

These data demonstrate that 19-substituted BQAs, which by design are incapable of arylation reactions, are markedly less hepatotoxic than their parent unsubstituted BQAs. Although this work still needs to be extended to *in vivo* studies, our mechanistic data suggests that arylation is a major mechanism responsible for hepatotoxicity. However, contributions of redox cycling to toxicity cannot be completely discounted since the studied compounds were still able to undergo one-electron reduction during liver microsome metabolism. This work indicates that the 19BQAs are less toxic than their parent quinones and if the Hsp90 inhibitory activity of this class of compounds can be maximized they may have a greater

MOL # 90654

therapeutic window than their unsubstituted parent compounds because of their inability to undergo arylation reactions.

We have previously defined the greater activity of the hydroquinone ansamycins towards inhibiting Hsp90 than their parent benzoquinone ansamycins. This is a result of a more favorable binding energy of the hydroquinone ansamycin in the Hsp90 active site, primarily due to increased hydrogen bonding (Guo et al., 2005). 19-Phenyl BQAs behaved in a similar fashion and retained their ability to inhibit purified Hsp90 in an NQO1-dependent manner, emphasizing the importance of the hydroquinone ansamycin in Hsp90 inhibition. The NQO1-dependence of 19-phenyl BQA-dependent Hsp90 inhibition translated to cellular studies, where greater Hsp90 inhibition was observed in MDA468/NQ16 breast cancer cells with elevated NQO1 levels, relative to isogenic NQO1-deficient cells. Furthermore, the growth inhibitory activity of 19Ph-DMAG could be abrogated using the NQO1 inhibitor ES936. 19-Phenyl BQAs caused degradation of Hsp90 client protein including Raf-1 and Akt and compensatory upregulation of Hsp70 to a greater extent in cells containing high NQO1 levels. However, growth inhibitory potency of these first generation 19-phenyl substituted compounds was not as great their parent quinones. To verify these molecules also have potential in HER2-expressing breast cancer cells, we also examined reduction of Hsp90 clients including HER2, induction of Hsp70 and growth

MOL # 90654

inhibitory effects in BT474 human breast cancer cells and marked growth inhibitory and Hsp90 inhibitory activity was observed with both 19Ph-DMAG and its parent quinone.

In summary, the limited series of 19BQAs that we have tested do not react with glutathione at the 19-position and exhibit reduced toxicity in primary mouse hepatocytes and a mouse hepatocyte cell line in comparison to their parent quinones. Furthermore, 19BQAs retain the ability to inhibit Hsp90 in both purified enzyme systems and in cellular systems. The development of 17-AAG and 17-DMAG as anti-cancer agents has recently been halted due to non-clinical reasons (Modi et al., 2011). This led to a pointed editorial asking why such active anticancer compounds, in trastuzumab resistant breast cancer for example, were no longer available (Arteaga, 2011). This leaves a void which novel, less toxic 19BQAs could conceivably fill. Clearly, optimization of the substituent at the 19-position needs to be performed for maximal inhibition of cellular Hsp90 and growth inhibitory potency, but data obtained with prototype 19-phenyl BQA compounds to demonstrate proof of principle suggests that this class of molecule is worthy of further translational investigation.

MOL # 90654

### **Acknowledgements**

The authors would like to acknowledge the contributions of the Computational Chemistry and Biology Core Facility at the University of Colorado Anschutz Medical Campus, which is supported in part by NIH/NCATS Colorado CTSI Grant UL1 TR001082.

### **Authorship Contributions**

Participated in research design: Chang, Drechsel, Siegel, Moody, Ju, and Ross

Conducted experiments: Chang, Drechsel, Siegel, You and Backos

Contributed new reagents or analytic tools: Kitson

Performed data analysis: Chang, Drechsel, and Siegel

Wrote or contributed to the writing of the manuscript: Drechsel, Chang, Moody, and

Ross

MOL # 90654

## References

- Arteaga CL (2011) Why is this effective HSP90 inhibitor not being developed in HER2+ breast cancer? *Clinical cancer research : an official journal of the American Association for Cancer Research* **17**(15): 4919-4921.
- Banerji U, O'Donnell A, Scurr M, Pacey S, Stapleton S, Asad Y, Simmons L, Maloney A, Raynaud F, Campbell M, Walton M, Lakhani S, Kaye S, Workman P and Judson I (2005) Phase I pharmacokinetic and pharmacodynamic study of 17-allylamino, 17-demethoxygeldanamycin in patients with advanced malignancies. *Journal of clinical oncology : official journal of the American Society of Clinical Oncology* **23**(18): 4152-4161.
- Beall HD, Mulcahy RT, Siegel D, Traver RD, Gibson NW and Ross D (1994) Metabolism of bioreductive antitumor compounds by purified rat and human DT-diaphorases. *Cancer research* **54**(12): 3196-3201.
- Cheng L, You Q, Yin H, Holt MP and Ju C (2010) Involvement of natural killer T cells in halothane-induced liver injury in mice. *Biochemical pharmacology* **80**(2): 255-261.
- Cysyk RL, Parker RJ, Barchi JJ, Jr., Steeg PS, Hartman NR and Strong JM (2006) Reaction of geldanamycin and C17-substituted analogues with glutathione: product identifications and pharmacological implications. *Chemical research*

MOL # 90654

*in toxicology* **19**(3): 376-381.

Dehn DL, Winski SL and Ross D (2004) Development of a new isogenic cell-xenograft system for evaluation of NAD(P)H:quinone oxidoreductase-directed antitumor quinones: evaluation of the activity of RH1. *Clin Cancer Res* **10**(15131056): 3147-3155.

Feig M and Brooks CL, 3rd (2004) Recent advances in the development and application of implicit solvent models in biomolecule simulations. *Current opinion in structural biology* **14**(2): 217-224.

Gartner EM, Silverman P, Simon M, Flaherty L, Abrams J, Ivy P and Lorusso PM (2012) A phase II study of 17-allylamino-17-demethoxygeldanamycin in metastatic or locally advanced, unresectable breast cancer. *Breast cancer research and treatment* **131**(3): 933-937.

Ge J, Normant E, Porter JR, Ali JA, Dembski MS, Gao Y, Georges AT, Grenier L, Pak RH, Patterson J, Sydor JR, Tibbitts TT, Tong JK, Adams J and Palombella VJ (2006) Design, synthesis, and biological evaluation of hydroquinone derivatives of 17-amino-17-demethoxygeldanamycin as potent, water-soluble inhibitors of Hsp90. *Journal of medicinal chemistry* **49**(15): 4606-4615.

Guo W, Reigan P, Siegel D and Ross D (2008) Enzymatic reduction and glutathione conjugation of benzoquinone ansamycin heat shock protein 90 inhibitors:



MOL # 90654

relevance for toxicity and mechanism of action. *Drug metabolism and disposition: the biological fate of chemicals* **36**(10): 2050-2057.

Guo W, Reigan P, Siegel D, Zirrolli J, Gustafson D and Ross D (2005) Formation of 17-allylamino-demethoxygeldanamycin (17-AAG) hydroquinone by NAD(P)H:quinone oxidoreductase 1: role of 17-AAG hydroquinone in heat shock protein 90 inhibition. *Cancer research* **65**(21): 10006-10015.

Guo W, Reigan P, Siegel D, Zirrolli J, Gustafson D and Ross D (2006) The bioreduction of a series of benzoquinone ansamycins by NAD(P)H:quinone oxidoreductase 1 to more potent heat shock protein 90 inhibitors, the hydroquinone ansamycins. *Mol Pharmacol* **70**(16825487): 1194-1203.

Kitson RR, Chang CH, Xiong R, Williams HE, Davis AL, Lewis W, Dehn DL, Siegel D, Roe SM, Prodromou C, Ross D and Moody CJ (2013) Synthesis of 19-substituted geldanamycins with altered conformations and their binding to heat shock protein Hsp90. *Nat Chem* **5**(4): 307-314.

Kitson RR and Moody CJ (2013) An improved route to 19-substituted geldanamycins as novel Hsp90 inhibitors--potential therapeutics in cancer and neurodegeneration. *Chemical communications* **49**(76): 8441-8443.

Koska J, Spassov VZ, Maynard AJ, Yan L, Austin N, Flook PK and Venkatachalam CM (2008) Fully automated molecular mechanics based induced fit

MOL # 90654

protein-ligand docking method. *Journal of chemical information and modeling* **48**(10): 1965-1973.

Lowry OH, Rosebrough NJ, Farr AL and Randall RJ (1951) Protein measurement with the Folin phenol reagent. *The Journal of biological chemistry* **193**(1): 265-275.

Modi S, Stopeck A, Linden H, Solit D, Chandarlapaty S, Rosen N, D'Andrea G, Dickler M, Moynahan ME, Sugarman S, Ma W, Patil S, Norton L, Hannah AL and Hudis C (2011) HSP90 inhibition is effective in breast cancer: a phase II trial of tanespimycin (17-AAG) plus trastuzumab in patients with HER2-positive metastatic breast cancer progressing on trastuzumab. *Clinical cancer research : an official journal of the American Association for Cancer Research* **17**(15): 5132-5139.

Neckers L and Workman P (2012) Hsp90 molecular chaperone inhibitors: are we there yet? *Clinical cancer research : an official journal of the American Association for Cancer Research* **18**(1): 64-76.

Normant E, Paez G, West KA, Lim AR, Slocum KL, Tunkey C, McDougall J, Wylie AA, Robison K, Caliri K, Palombella VJ and Fritz CC (2011) The Hsp90 inhibitor IPI-504 rapidly lowers EML4-ALK levels and induces tumor regression in ALK-driven NSCLC models. *Oncogene* **30**(22): 2581-2586.

MOL # 90654

- Pacey S, Wilson RH, Walton M, Eatock MM, Hardcastle A, Zetterlund A, Arkenau HT, Moreno-Farre J, Banerji U, Roels B, Peachey H, Aherne W, de Bono JS, Raynaud F, Workman P and Judson I (2011) A phase I study of the heat shock protein 90 inhibitor alvespimycin (17-DMAG) given intravenously to patients with advanced solid tumors. *Clinical cancer research : an official journal of the American Association for Cancer Research* **17**(6): 1561-1570.
- Pearl LH and Prodromou C (2006) Structure and mechanism of the Hsp90 molecular chaperone machinery. *Annu Rev Biochem* **75**: 271-294.
- Rajan A, Kelly RJ, Trepel JB, Kim YS, Alarcon SV, Kummar S, Gutierrez M, Crandon S, Zein WM, Jain L, Mannargudi B, Figg WD, Houk BE, Shnaidman M, Brega N and Giaccone G (2011) A phase I study of PF-04929113 (SNX-5422), an orally bioavailable heat shock protein 90 inhibitor, in patients with refractory solid tumor malignancies and lymphomas. *Clinical cancer research : an official journal of the American Association for Cancer Research* **17**(21): 6831-6839.
- Ross D, Kepa JK, Winski SL, Beall HD, Anwar A and Siegel D (2000) NAD(P)H:quinone oxidoreductase 1 (NQO1): chemoprotection, bioactivation, gene regulation and genetic polymorphisms. *Chemico-biological interactions* **129**(1-2): 77-97.

MOL # 90654

Siegel D, Jagannath S, Vesole DH, Borello I, Mazumder A, Mitsiades C, Goddard J,

Dunbar J, Normant E, Adams J, Grayzel D, Anderson KC and Richardson P

(2011) A phase 1 study of IPI-504 (retaspimycin hydrochloride) in patients

with relapsed or relapsed and refractory multiple myeloma. *Leukemia &*

*lymphoma* **52**(12): 2308-2315.

Siegel D, Kepa JK and Ross D (2007) Biochemical and genetic analysis of

NAD(P)H:quinone oxidoreductase 1 (NQO1). *Curr Protoc Toxicol* **Chapter 4:**

Unit4 22.

Solit DB, Ivy SP, Kopil C, Sikorski R, Morris MJ, Slovin SF, Kelly WK, DeLaCruz A,

Curley T, Heller G, Larson S, Schwartz L, Egorin MJ, Rosen N and Scher HI

(2007) Phase I trial of 17-allylamino-17-demethoxygeldanamycin in patients

with advanced cancer. *Clinical cancer research : an official journal of the*

*American Association for Cancer Research* **13**(6): 1775-1782.

Sreeramulu S, Gande SL, Gobel M and Schwalbe H (2009) Molecular mechanism of

inhibition of the human protein complex Hsp90-Cdc37, a kinome

chaperone-cochaperone, by triterpene celastrol. *Angew Chem Int Ed Engl*

**48**(32): 5853-5855.

Supko JG, Hickman RL, Grever MR and Malspeis L (1995) Preclinical pharmacologic

evaluation of geldanamycin as an antitumor agent. *Cancer chemotherapy and*

MOL # 90654

*pharmacology* **36**(4): 305-315.

Whitesell L and Lindquist SL (2005) HSP90 and the chaperoning of cancer. *Nat Rev*

*Cancer* **5**(10): 761-772.

Whitesell L, Mimnaugh EG, De Costa B, Myers CE and Neckers LM (1994)

Inhibition of heat shock protein HSP90-pp60v-src heteroprotein complex formation by benzoquinone ansamycins: essential role for stress proteins in oncogenic transformation. *Proc Natl Acad Sci U S A* **91**(18): 8324-8328.

Workman P (2004) Combinatorial attack on multistep oncogenesis by inhibiting the

Hsp90 molecular chaperone. *Cancer Lett* **206**(2): 149-157.

Workman P, Burrows F, Neckers L and Rosen N (2007) Drugging the cancer

chaperone HSP90: combinatorial therapeutic exploitation of oncogene addiction and tumor stress. *Annals of the New York Academy of Sciences* **1113**: 202-216.

Wu JC, Merlino G, Cveklova K, Mosinger B, Jr. and Fausto N (1994) Autonomous

growth in serum-free medium and production of hepatocellular carcinomas by differentiated hepatocyte lines that overexpress transforming growth factor alpha 1. *Cancer research* **54**(22): 5964-5973.

Yin H, Cheng L, Holt M, Hail N, Jr., Maclaren R and Ju C (2010) Lactoferrin protects

against acetaminophen-induced liver injury in mice. *Hepatology* **51**(3):

MOL # 90654

1007-1016.

MOL # 90654

### **Footnotes**

C-H.C. and D.A.D. contributed equally to this work.

This work was supported by National Institutes of Health National Cancer Institute

[Grant CA51210] (D.R.) and the Parkinson's Disease Society UK (C.J.M.)

MOL # 90654

## **Legends for Figures**

### **Figure 1.**

#### **Chemical structures of BQAs and 19-substituted BQAs.**

### **Figure 2.**

#### **19-Substitution of BQAs prevents GSH conjugation.**

HPLC analysis of the formation of BQA- and 19BQA-glutathione conjugates. Briefly, 50  $\mu$ M BQAs, 19Ph BQAs, or 19Me-BQAs, 500  $\mu$ M NADH, and 5 mM glutathione were incubated in 50 mM potassium phosphate buffer (pH 7.4, 1 ml) at room temperature for 15 min (GA series), 3 h (17-DMAG series), or 16 h (17-AAG series). Following incubation, concentrations of unconjugated BQA and 19BQAs were measured by HPLC at 270 nm. Data expressed as mean  $\pm$  SEM (n = 3) of remaining BQA or 19BQA concentration following incubation. Solid bars represent samples run in the absence of minus glutathione, while dashed bars represent sample run in the presence of glutathione. \* p < 0.05 versus corresponding sample with no glutathione (two-tailed t-test).

### **Figure 3.**

#### **Redox cycling of BQAs and 19BQAs by mouse and human liver microsomes.**



MOL # 90654

The redox cycling rates of BQAs and 19BQAs were determined in human (A, B) and mouse (C, D) liver microsomes supplied with NADH or NADPH by measuring the rates of oxygen consumption as described in Experimental Methods. The naphthoquinone menadione was used as a positive control in these experiments. Data expressed as mean  $\pm$  SEM (n = 3). \* p < 0.05 versus parent BQA for each 19BQA (one-way ANOVA with Tukey's post-test).

**Figure 4.**

**19-Substituted BQAs show reduced hepatotoxicity compared to parent quinones.**

Hepatocytes were isolated from naïve male C57BL/6 mice and cultured in 96-well plates ( $1 \times 10^4$  cells/well). The cells were treated with increasing concentrations of 17-DMAG, 19Ph-DMAG, or 19Me-DMAG for 24 h. DMSO-treated cells served as control. (A) Cell viability and (B) cytotoxicity was determined using MTT and AST release assays, respectively, as described in Experimental Methods. Data expressed as mean  $\pm$  SEM (n = 4-8). Dashed line in (B) represents AST activity in DMSO-treated cells. \* p < 0.05 versus untreated (DMSO) control, # p < 0.05 versus 17-DMAG at same concentration (one-way ANOVA with Tukey's post-test).

**Figure 5.**

MOL # 90654

### **Inhibition of yeast Hsp90 ATPase activity by BQAs and 19-phenyl BQAs.**

Yeast Hsp90 ATPase activity was measured in reactions with either vehicle (DMSO), BQAs, or 19BQAs at indicated concentrations in the presence or absence of rhNQO1. The reactions were analyzed after 3 h, and phosphate concentrations were measured using the malachite green assay. Solid bars represent samples run in absence of rhNQO1, while dashed bars represent samples run in presence of rhNQO1. Data expressed as mean  $\pm$  SEM (n = 3). \* p < 0.05 versus corresponding sample without rhNQO1 (two-tailed t-test).

### **Figure 6.**

#### **Effect of NQO1 inhibition on 19Ph-DMAG-dependent growth inhibition in human breast cancer cells.**

MDA468 cells lacking NQO1 activity or isogenic MDA468/NQ16 cells containing human NQO1 were pretreated with ES936 (100 nM) to inhibit NQO1 activity for 30 min prior to 19Ph-DMAG treatment. Growth inhibition with 4 hr 19Ph-DMAG treatment followed by 72 h drug-free incubation was determined via MTT analysis. Data expressed as mean  $\pm$  SEM (n = 4). \* p < 0.05 versus same cell type with ES936 pretreatment (two-way ANOVA with concentration-group interaction for multiple comparisons).

MOL # 90654

**Figure 7.**

**Effect of 17-DMAG and 19Ph-DMAG on Hsp90 client proteins and heat shock protein induction in human breast cancer cells is NQO1 dependent**

Immunoblot analysis of Hsp90 client protein degradation (Raf-1 and Akt) and Hsp70 compensatory response in MDA468/NQ16 (A) and MDA468 cells (C) treated with 17-DMAG and 19Ph-DMAG at 5  $\mu$ M for 24 h. DMSO-treated cells served as control. Blots are representative of three independent experiments. (B, D) Fold change of the indicated proteins are normalized to DMSO control and estimated by densitometry. Data expressed as mean  $\pm$  SEM (n = 3) \* p < 0.05 versus DMSO, # p < 0.05 versus 17-DMAG (one-way ANOVA with Tukey's post-test).

**Figure 8.**

**19Ph-DMAG inhibits growth in HER2-positive human breast cancer cells with molecular signatures of Hsp90 inhibition.**

(A) Growth inhibition following either 17-DMAG or 19Ph-DMAG treatment was measured by MTT analysis in BT474 cell lines. Data expressed at mean  $\pm$  SEM (n = 3). (B) Immunoblot analysis of Hsp90 client proteins (HER2, Raf-1 and Akt) and Hsp70 compensatory response in BT474 cells treated with either 17-DMAG or

MOL # 90654

19Ph-DMAG at 5  $\mu$ M for 24 h. Blots are representative of three independent experiments. (C) Fold change of the indicated proteins are normalized to DMSO control and estimated by densitometry. Data expressed as mean  $\pm$  SEM (n = 3) \* p < 0.05 versus DMSO, # p < 0.05 versus 17-DMAG (one-way ANOVA with Tukey's post-test).

MOL # 90654

**Table 1.**

**Hepatotoxicity of Hsp90 inhibitors in the TAMH cell line.**

<b>Compound</b>	<b>IC<sub>50</sub> (μM)</b>	<b>LC<sub>50</sub> (μM)</b>
17-DMAG	0.02 ± 0.01	0.21 ± 0.01
19Ph-DMAG	4.61 ± 0.39	13.83 ± 3.57
19Me-DMAG	8.00 ± 0.37	42.67 ± 0.16

Data expressed as mean ± standard deviation of three independent experiments.

MOL # 90654

**Table 2.**

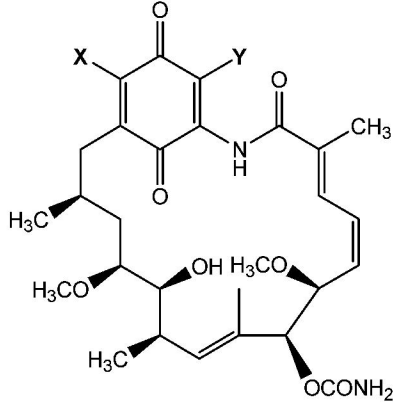
**Growth inhibition induced by Hsp90 inhibitors in human breast cancer cell lines**

**dependent upon NQO1 activity**

Compound	IC <sub>50</sub> (μM)		IC <sub>50</sub> -fold difference
	MDA468	MDA468/NQ16	
GA	0.06 ± 0.01	0.02 ± 0.01	3.00
19Ph-GA	7.45 ± 0.51	1.19 ± 0.08	6.30
17-AAG	10.05 ± 1.07	0.86 ± 0.16	11.70
19Ph-AAG	88.37 ± 2.46	38.79 ± 10.90	2.27
17-DMAG	0.61 ± 0.02	0.19 ± 0.02	3.15
19Ph-DMAG	16.48 ± 2.14	3.28 ± 0.26	5.02

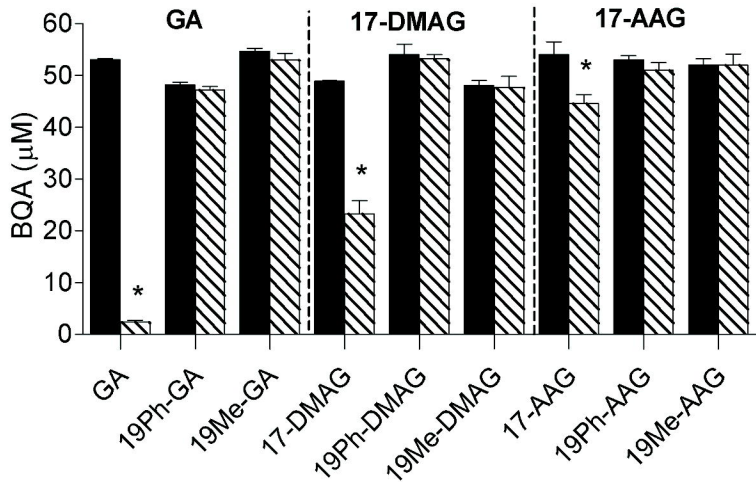
Data expressed as mean ± standard deviation of three independent experiments.

**Figure 1**



Compound	X	Y
<b>GA</b>	OCH <sub>3</sub>	H
<b>19Ph-GA</b>	OCH <sub>3</sub>	phenyl
<b>19Me-GA</b>	OCH <sub>3</sub>	methyl
<b>17-AAG</b>	NHCH <sub>2</sub> CHCH <sub>2</sub>	H
<b>19Ph-AAG</b>	NHCH <sub>2</sub> CHCH <sub>2</sub>	phenyl
<b>19Me-AAG</b>	NHCH <sub>2</sub> CHCH <sub>2</sub>	methyl
<b>17-DMAG</b>	NHCH <sub>2</sub> CH <sub>2</sub> N(CH <sub>3</sub> ) <sub>2</sub>	H
<b>19Ph-DMAG</b>	NHCH <sub>2</sub> CH <sub>2</sub> N(CH <sub>3</sub> ) <sub>2</sub>	phenyl
<b>19Me-DMAG</b>	NHCH <sub>2</sub> CH <sub>2</sub> N(CH <sub>3</sub> ) <sub>2</sub>	methyl

**Figure 2**





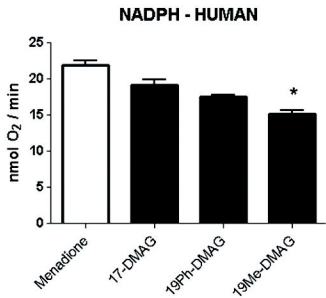
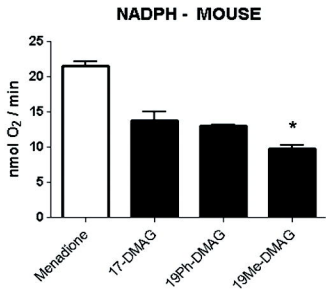
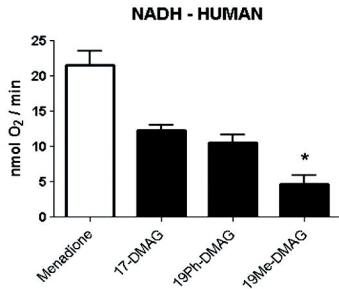
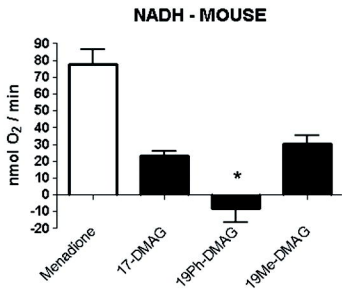
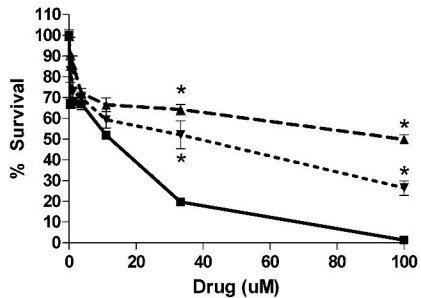
**Figure 3****A****B****C****D**

Figure 4

A



B

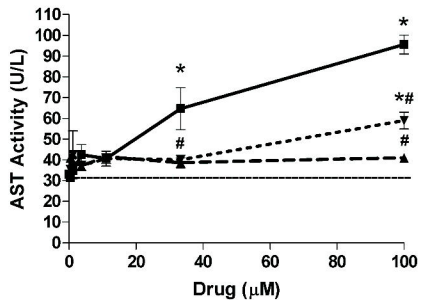


Figure 5

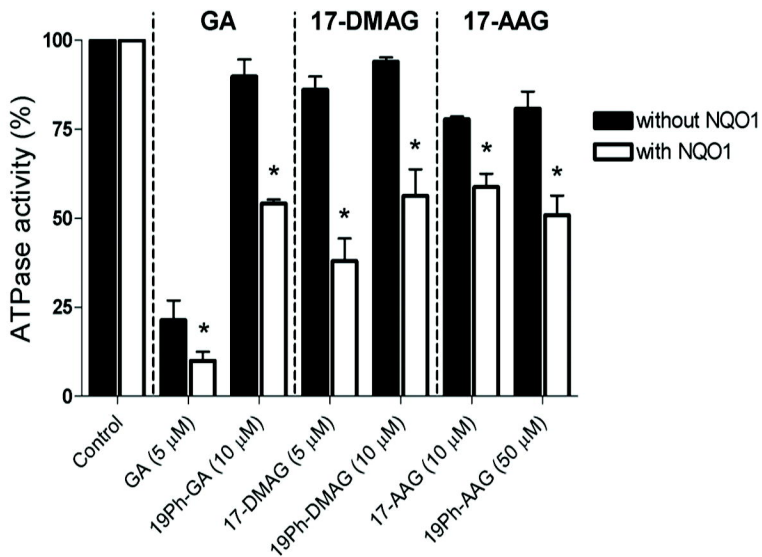


Figure 6

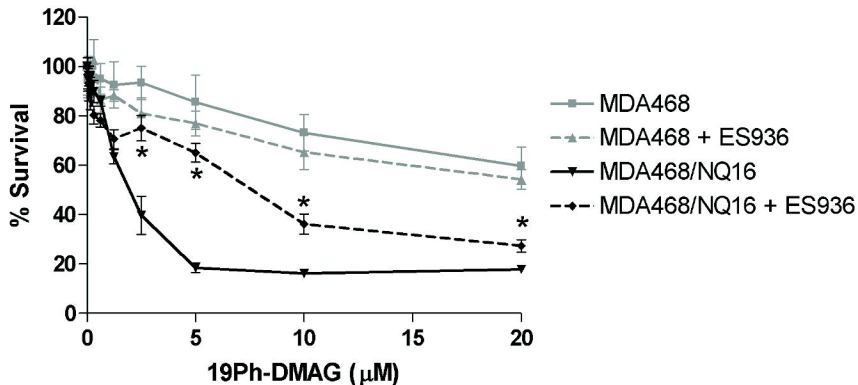


Figure 7

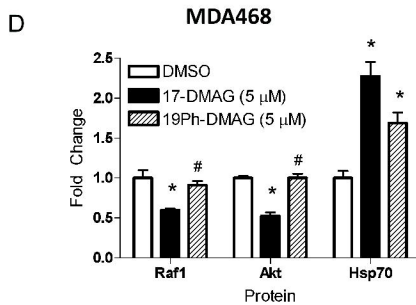
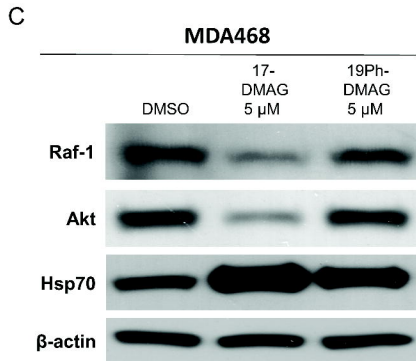
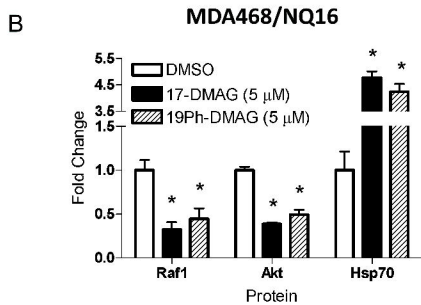
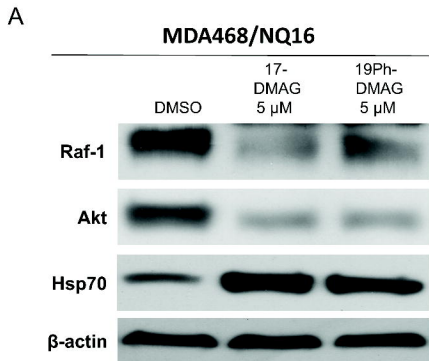
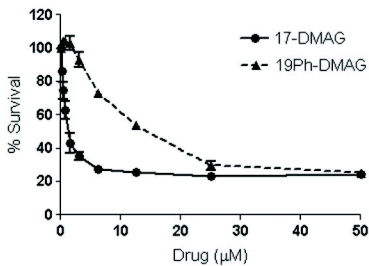
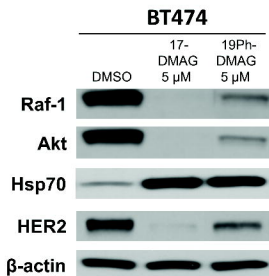


Figure 8

A



B



C

